

## Density functional study of the effect of pressure on the ferroelectric GeTe

Adrian Ciucivara,<sup>1</sup> B. R. Sahu,<sup>2</sup> and Leonard Kleinman<sup>1</sup>

<sup>1</sup>*Department of Physics, University of Texas at Austin, Austin, Texas 78712, USA*

<sup>2</sup>*Microelectronics Research Center, University of Texas at Austin, Austin, Texas 78758, USA*

(Received 13 January 2006; revised manuscript received 12 April 2006; published 7 June 2006)

We compare local density approximation (LDA) and generalized gradient approximation (GGA) calculations of GeTe as a function of applied pressure. The LDA yields a fair result for the zero pressure trigonal angle but good to excellent results for the zero pressure lattice constant, energy gap, and relative positions of the two sublattices. More importantly, it yields results within the wide range of experimental values for the critical pressure at which the ferroelectric trigonal to rock salt transition takes place. We also obtain very reasonable results for the zero pressure cohesive energy, electric polarization, and Born effective charge, for which there are no experimental data. Except for the energy gap which is more than a factor of 2 too large, the GGA results are slightly better than the LDA.

DOI: [10.1103/PhysRevB.73.214105](https://doi.org/10.1103/PhysRevB.73.214105)

PACS number(s): 77.80.Bh, 77.84.Bw

Ferroelectric crystals find a multiplicity of technological functions; their pyroelectric nature is used in thermal and infrared sensors. In BaTiO<sub>3</sub> and some other ferroelectrics, light induces changes in the refracting indices, which is used for information storage and real-time optical processors. Their high dielectric constants make them candidates to replace SiO<sub>2</sub> in metal-oxide-semiconductor devices. Those that are piezoelectrics find numerous applications in electromechanical transducers. Some can be used for reversible phase change optical data storage. For example, stoichiometric films of GeTe can be crystallized with laser pulses of less than 100 ns duration.<sup>1</sup>

Having only two atoms per unit cell, GeTe is undoubtedly the simplest ferroelectric. Above about 720 K it crystallizes in the rock salt structure,<sup>2</sup> as do many of the other IV-VI compounds such as PbTe, SnTe, PbSe, etc. It is the only one (at about 720 K) to undergo a displacive transition to a trigonal (rhombohedral) structure consisting of an inner displacement along a [111] direction with a corresponding [111] stretch of the lattice. Using a model Hamiltonian with parameters obtained from self-consistent density functional calculations, Rabe and Joannopoulos<sup>3</sup> predicted a transition temperature of 657±100 K. There is a long history of the pressure induced phase transition at room temperature but no calculations of the critical pressure of which we are aware. The experimental value is extremely sensitive to any shear component in the applied pressure.<sup>4,5</sup> Kabalkina *et al.*<sup>6</sup> obtained a 3.5 GPa critical pressure accompanied by a sudden 3% decrease in volume. Using silicone grease, a nonhydrostatic pressure transmitting medium, Leger and Redon<sup>4</sup> obtained a transition around 4 GPa with no volume discontinuity. Using a liquid 4:1 methanol-ethanol medium they found that the rhombohedral phase persisted up to 8 GPa, the maximum investigated pressure. Nevertheless, Onodera *et al.*<sup>7</sup> find that the transition occurs at 3 GPa (with no volume discontinuity).

A simple physical picture for the restoration of the rock salt structure under pressure is as follows. The sublattice displacements shorten three of the six nearest neighbor bonds while lengthening the other three. Under pressure the long bonds are easily compressed while the short bonds are

not. As the pressure is increased and the bond lengths become more equal, at some point it becomes energetically favorable to go to complete equality and for the trigonal distortion, which was driven by the sublattice displacements, to vanish. A somewhat different explanation was given by Kornev *et al.*<sup>8</sup> They say that ferroelectricity results from a delicate balance between long range Coulomb ionic interactions favoring ferroelectric distortions and short range electronic effects preferring the undistorted paraelectric cubic structure and that the balance can be tipped towards ferroelectricity by small covalent effects.

Because there is some evidence that the energy gap of GeTe has a relatively strong dependence on spin-orbit coupling,<sup>9</sup> we have performed fully relativistic calculations of the electronic structure of GeTe using the projected augmented wave method<sup>10</sup> (PAW) as implemented in the VASP software package.<sup>11</sup> The exchange-correlation density functional was calculated in both the local density approximation (LDA) and the PBE (Ref. 12) form of the generalized gradient approximation (GGA). A 20×20×20 *k*-point mesh was used in the Brillouin zone (BZ) which was integrated over using the quadratic tetrahedron scheme.<sup>13</sup> We expanded in all plane waves with an energy below 21 Ry and reduced the force on the displaced sublattices to less than 1.5 meV/Å. Our convergence at the LDA equilibrium volume is displayed in Table I. We reduced the force criterion<sup>14</sup> from 1.5 to 0.3 meV/Å, which increased the cohesive energy by 0.059 meV. Because we are interested in the energy differences between the cubic and trigonal structures and there are

TABLE I. Convergence of the cohesive energy at the trigonal phase equilibrium volume with a decrease in the maximum force, an increase in the plane wave energy cutoff, and an increase in the number of BZ mesh points.

<i>k</i> mesh	pw (Ry)	(meV/Å)	$E_c$ (eV)	$\Delta E_c$ (meV)
20×20×20	21	1.5	7.769030	
20×20×20	21	0.3	7.769089	0.059
20×20×20	32	0.3	7.769382	0.293
26×26×26	32	0.3	7.769509	0.127

TABLE II. Comparison of LDA and GGA trigonal GeTe results with experiment, all at 1 atm pressure except for  $p_c$ , the critical pressure for the rhombohedral to rock salt transition.  $\Omega$  is the unit cell volume,  $a$  and  $\alpha$  the cubic lattice constant and angle, i.e.,  $\Omega=(a^3/4)\sin^2\alpha$ ,  $E_{\text{coh}}$  is the cohesive energy,  $B$  is the bulk modulus,  $\tau$  is the deviation from  $0.5a$  of the displacement of the Ge sublattice from the Te sublattice,  $E_{\text{gap}}$  is the indirect energy gap, and  $P$  is the polarization.

	$\Omega$ ( $\text{\AA}^3$ )	$a$ ( $\text{\AA}$ )	$\alpha$ ( $^\circ$ )	$E_{\text{coh}}$ (eV)	$B$ (GPa)	$\tau(a)$	$E_{\text{gap}}$ (meV)	$P$ ( $\mu\text{C cm}^{-2}$ )	$p_c$ (GPa)
LDA	50.96	5.886	89.24	7.77	37.64	0.0217	209	61.13	5.313
GGA	55.96	6.074	88.06	6.46	32.70	0.0304	469	64.90	8.448
Exp	53.31 <sup>a</sup>	5.98 <sup>a</sup>	88.35 <sup>a</sup>		49.9 <sup>b</sup>	0.0248 <sup>a</sup>	200 <sup>c</sup>		3 <sup>b</sup>
Exp <sup>d</sup>		5.986	88.59		<38.3				>8

<sup>a</sup>Reference 5.

<sup>b</sup>Reference 7.

<sup>c</sup>Reference 18.

<sup>d</sup>Reference 4.

no forces in the cubic case, as well as the fact that the other convergence properties are expected to be similar for the two structures, this 0.059 meV may be more significant than the 0.293 meV gained by increasing the plane wave cutoff energy from 21 to 32 Ry. The increase of 0.127 meV on increasing the  $k$ -point sampling from  $20 \times 20 \times 20$  to  $26 \times 26 \times 26$  may also be similar in the trigonal and cubic cases. In Table II are listed all the important results of our calculations. After discussing these we will go into somewhat more

detail for the LDA case (the GGA is similar and yields no additional physics) using the data in Table III. The first column compares the rhombohedral unit cell volumes, which are smaller (LDA) and larger (GGA) than experiment. The larger discrepancy with experiment (LDA) of the ‘‘cubic’’ lattice constants is less than 2%. Experimental papers do not as a rule give a value for the trigonal lattice constant.<sup>15</sup> The second column compares the angle between two cubic lattice vectors. Again, the LDA and GGA results are on opposite

TABLE III. The LDA trigonal lattice constant, angle, and sublattice displacement as a function of 1% deviations from the trigonal cell equilibrium volume. The next three columns list the trigonal and rock salt cohesive energies and their differences, the next two list the trigonal and rock salt indirect energy gaps, and the last column lists the pressure acting on the trigonal crystal, all as a function of the unit cell volume.

	$\Omega$ ( $\text{\AA}^3$ )	$a$ ( $\text{\AA}$ )	$\alpha$ ( $^\circ$ )	$\tau(a)$	$E_c^{\text{trig}}$ (eV)	$E_c^{\text{cube}}$ (eV)	$\Delta E$ (meV)	$E_g^{\text{trig}}$ (meV)	$E_g^{\text{cube}}$ (meV)	$p$ (GPa)
5%	53.5080	5.9830	88.55	0.027434	7.75594	7.72754	28.395	411.7	205.3	
4%	52.9984	5.9636	88.74	0.025900	7.76113	7.73674	24.390	379.2	175.5	-1.270
3%	52.4888	5.9443	88.86	0.024764	7.76523	7.74449	20.747	340.2	144.7	-0.841
2%	51.9792	5.9248	88.97	0.023500	7.76716	7.75067	16.489	311.8	112.8	-0.609
1%	51.4696	5.9053	89.11	0.022132	7.76791	7.75524	12.663	282.2	80.0	-0.320
0%	50.9601	5.8856	89.24	0.021681	7.76903	7.75907	9.966	208.7	1.8	0.009
-1%	50.4504	5.8657	89.35	0.019422	7.76793	7.75909	8.846	195.1	11.4	0.593
-2%	49.9408	5.8459	89.41	0.018097	7.76572	7.75821	7.511	174.2	24.5	1.158
-3%	49.4312	5.8260	89.43	0.016606	7.75969	7.75424	5.450	138.8	61.1	1.754
-4%	48.9216	5.8058	89.58	0.015245	7.75454	7.74940	5.137	79.4	45.6	2.371
-5%	48.4120	5.7855	89.64	0.013681	7.74524	7.74231	2.928	43.1	12.4	3.012
-6%	47.9024	5.7651	89.71	0.012195	7.73478	7.73298	1.807	35.3	-11.5	3.684
-7%	47.3928	5.7446	89.78	0.010536	7.72209	7.72115	0.938	28.4	-18.3	4.394
-8%	46.8832	5.7239	89.85	0.008513	7.70706	7.70678	0.284	11.0	-42.3	5.141
-9%	46.3736	5.7031	89.94	0.004216	7.68963	7.68972	-0.094	-76.0	-80.5	5.923
-10%	45.8640	5.6822	89.96	0.000653	7.66971	7.66979	-0.076	-95.0	-119.5	6.742
-11%	45.3544	5.6610	89.98	0.000470	7.64673	7.64680	-0.071	-163.0	-159.5	7.614
-12%	44.8448	5.6397	89.97	0.000201	7.62055	7.62064	-0.082	-196.6	-200.6	8.575
-13%	44.3352	5.6183	89.96	0.000077	7.59292	7.59296	-0.042	-240.2	-241.5	9.672
-14%	43.8256	5.5967	89.95	0.000030	7.55982	7.55988	-0.059	-279.1	-281.8	10.940
-15%	43.3160	5.5749	89.95	0.000013	7.52279	7.52283	-0.035	-330.5	-332.6	12.340
-16%	42.8064	5.5529	89.96	0.000004	7.48180	7.48184	-0.045	-396.6	-398.2	

sides of the experimental values. There are no experimental values for the GeTe cohesive energy but comparing with the sum of the Ge and Te cohesive energies<sup>16</sup> (6.04 eV) we see that our calculated values<sup>17</sup> indicate that GeTe is stable against phase separation. The bulk moduli in the fifth column were obtained from a three point fit. A five point Vinet<sup>18</sup> fit for the LDA (GGA) case yields 34.908 GPa (33.216 GPa) while an eleven point fit yields 43.436 GPa (30.024 GPa) closely bracketing the three point GGA result and also bracketing the LDA result, but not as closely. It has been our<sup>19</sup> experience that discrepancies within an equation of state (EOS) due to a fitting at a different number of points are much larger than discrepancies between different EOS. The less than 38.36 GPa quoted from Ref. 3 is deduced from the statement that the GeTe bulk modulus is less than that of<sup>16</sup> Sb. The sixth column lists the deviation of the separation of the Ge and Te sublattices away from  $0.5a$ . The LDA and GGA results are close to and on opposite sides of the experimental value. The seventh column lists the indirect energy gap, which is between the  $L$  point and the point at  $(0.35, 0.2, 0.2)$  along the trigonal reciprocal lattice vectors for both LDA and GGA. Ignoring the small trigonal distortion, this would be the  $(0.05, 0.35, 0.35)$  point in the fcc BZ. The LDA gap is in near perfect agreement with the value of 200 meV obtained from tunneling spectroscopy.<sup>20</sup> The GGA gap is much too large; it appears that the gap is very strongly coupled to the deviation of  $\alpha$  from  $90^\circ$ . Note that the GGA/LDA gap ratio is 2.55. Although this gap discrepancy could be attributed to the larger GGA equilibrium volume, note that (in Table III) the rock salt structure has a gap of only 1.8 meV at the trigonal equilibrium volume. The direct gap at  $L$  is 369 meV (LDA) and 685 meV (GGA). The direct gap at  $Z$ , which would be the fourth  $L$  point in the fcc BZ, is even wider: 429 meV for LDA and 1054 meV for GGA. The LDA energy bands on the reflection plane are displayed in Fig. 1. The notation of Slater<sup>21</sup> is used for the symmetry points except for  $U$ , the point at which the rectangular and hexagonal faces of the BZ meet, because it has no symmetry beyond the reflection. It corresponds to the fcc  $U$  point. Using the Berry phase formula for the zero electric field polarization<sup>22</sup> as implemented in VASP,<sup>10</sup> we obtained the values listed in the seventh column. For the LDA,  $\mathbf{P}=61.13 \mu\text{C cm}^{-2}$ . The Berry phase calculation of the polarization has an uncertainty of

$$\Delta\mathbf{P} = (2e/\Omega) \sum_{n=1}^5 \mathbf{R}_n,$$

where the sum is over the energy bands and  $\mathbf{R}_n$  is a lattice vector in the direction of the polarization.<sup>22</sup> Taking one of the  $\mathbf{R}_n$  to be the shortest (111) lattice vector and the rest to be zero, we obtain a minimum LDA  $\Delta\mathbf{P}$  of  $648 \mu\text{C cm}^{-2}$ . This represents the translation of one band of electrons through  $\mathbf{R}_n$  and results in the next to smallest LDA value of  $\mathbf{P}$  being  $-587 \mu\text{C cm}^{-2}$ , which is clearly unphysical. It is surprising that the LDA and GGA yield such similar results, considering their large difference in  $(90^\circ - \alpha)$  and in the sublattice displacement  $\tau$ . There are no experimental values for GeTe but our calculated values are surprisingly large, agreeing

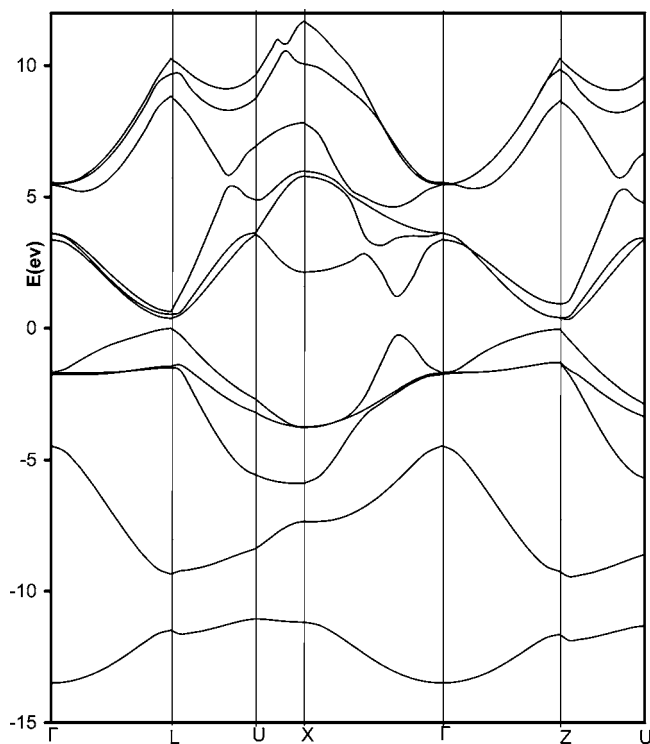


FIG. 1. Energy bands of rhombohedral GeTe. The zero of energy was taken at the top of the valence band.

very well with the largest experimental values found in other displacive ferroelectrics such as<sup>16</sup>  $\text{LiTaO}_3$  ( $50 \mu\text{C cm}^{-2}$ ),  $\text{PbTiO}_3$  ( $>50 \mu\text{C cm}^{-2}$ ), and  $\text{LiNbO}_3$  ( $71 \mu\text{C cm}^{-2}$ ).

The Born effective charge<sup>23,24</sup>  $Z^*$  is obtained from  $Z^*e = \Omega(\Delta P/\Delta\tau)$ . We took  $\Delta\tau$  to be  $0.1\tau$  and calculated the polarization with  $\tau$  replaced by  $0.9\tau$ , keeping the lattice constants fixed. The numerical values needed to evaluate  $Z^*$  are given in Table IV.  $P_{\text{xtrp}}$  is the polarization extrapolated from  $0.9\tau$  to  $\tau$ ,  $P_{\text{xtrp}} = P(0.9\tau)/0.9$ . The ratio  $P_{\text{xtrp}}/P(\tau)$  is also listed to demonstrate the nonlinearity of  $P$  with  $\tau$ . The large values of  $Z^*$  were to be expected because of the large values of the polarization, which are sufficient, but not necessary, to obtain large  $Z^*$ 's.<sup>25</sup> There are no experimental values but if one makes the geometric extrapolation  $8.1/6.5 = Z^*/8.1$ , where 6.5 and 8.1 are the experimental<sup>23</sup> values for  $\text{PbTe}$  and  $\text{SnTe}$ , one obtains  $Z^* = 10.09$ , in remarkable agreement with our LDA result. Tanaka and Shindo<sup>23</sup> obtained  $Z^* = 7.7$  from an empirical pseudopotential calculation. Further insight into the reason for the large value of  $Z^*$  may be obtained from plots of the pseudocharge density along the nearest neighbor direction in Fig. 2 and along the three-fold axis in Fig. 3. In

TABLE IV. The polarization at the equilibrium lattice constant, evaluated at the equilibrium value of  $\tau$  and at  $0.9\tau$ , and their difference, all in  $\mu\text{C cm}^{-2}$ , and  $\Delta\tau = 0.1\tau$ , in  $\text{\AA}$ , and the effective charge  $Z^*$ . The last columns compare the extrapolated values of  $P$  to  $P(\tau)$ .

	$P(\tau)$	$P(0.9\tau)$	$\Delta P$	$\Delta\tau$ ( $\text{\AA}$ )	$Z^*$	$P_{\text{xtrp}}/P(\tau)$
LDA	61.13	57.07	4.06	0.0127	10.11	1.037
GGA	64.90	59.46	5.44	0.0185	10.25	1.018

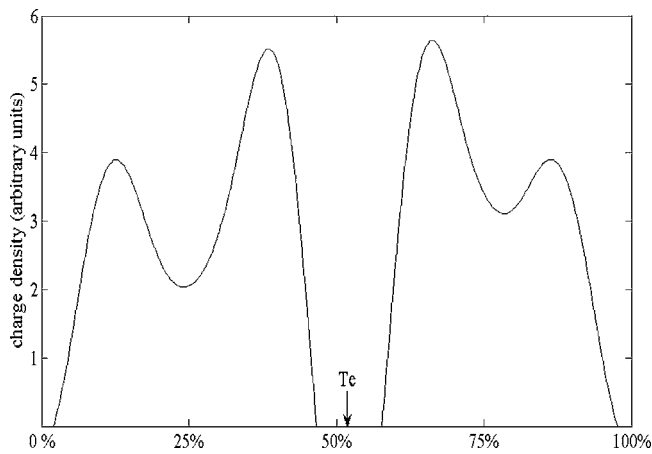


FIG. 2. Plot of the pseudocharge density along the nearest neighbor direction in trigonal GeTe. The Te atom is where indicated while the Ge atoms are at 0% and 100%. An artifact of the VASP PAW code is that it produces negative pseudocharge densities in the atomic cores. The negative values are here set equal to zero.

Fig. 2 we see extremely strong covalent bonding and the shorter bond is stronger (i.e., it has a shallower minimum in the bond) than the longer bond, which was to be expected. The plot along the 3-fold axis is much more interesting. Extrapolating from this one-dimensional picture to three dimensions, we note that both atoms are polarized with their larger charge density peaks on the long bond side of the atoms. This means that rather than moving with the ions and screening out a part of their contribution, the electrons move in the opposite direction and add to both the polarization and  $Z^*$ . The calculated transition pressures in the last column of Table II lie within the large range of experimental values. This large difference between the experimental results could be due to different sample stoichiometries. We note that the sample used in Ref. 20 had  $2 \times 10^{20}$  holes per  $\text{cm}^3$ , indicating a similar density of vacancies or impurities.

Figure 4 is a plot of the LDA cohesive energy of the trigonal and rock salt structures as a function of the unit cell volume whose values are listed in Table III. Note that the curves in Fig. 4 represent the raw data with no smoothing.

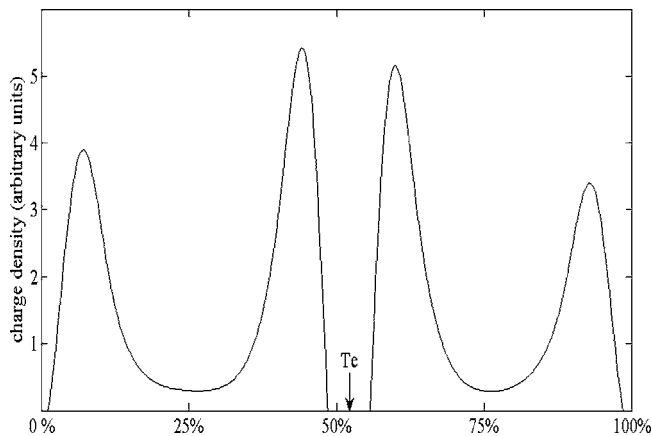


FIG. 3. Identical to Fig. 2 except that the plot is along the three-fold axis.

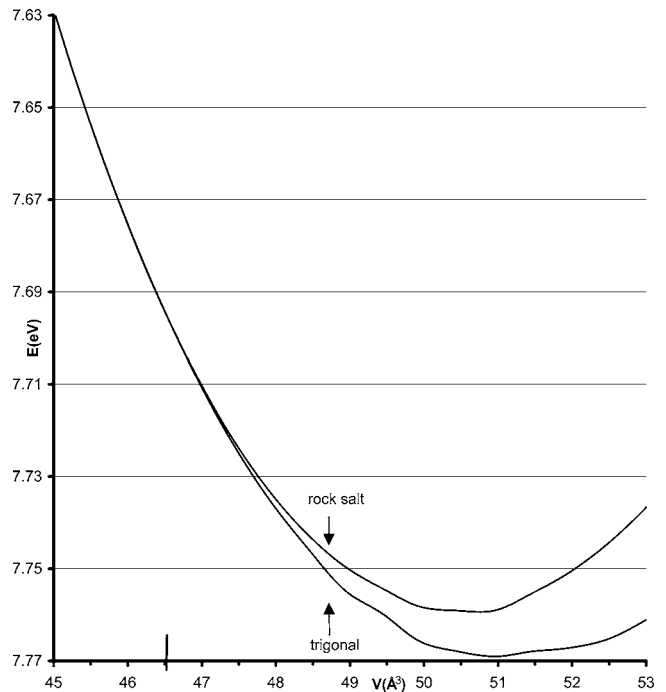


FIG. 4. Cohesive energy vs volume plots for rock salt and rhombohedral GeTe. The large tick mark indicates the volume at which the curves cross.

The trigonal curve is less smooth than the rock salt because for a fixed volume the trigonal energy must be minimized with respect to  $\alpha$  and  $\tau$  whereas the rock salt energy has no parameter dependence. As far as one can tell from Fig. 4 the transition is second order, in agreement with Onodera *et al.*<sup>7</sup> We note that the transition occurs just after the trigonal indirect energy gap becomes negative, i.e., just after trigonal GeTe becomes a semimetal. The same is true for the GGA calculation even though it occurs at a considerably higher pressure. This leads us to believe that this is cause and effect rather than coincidence. Of course, because of the screening by the conduction electrons, a metal cannot be ferroelectric. However, there is no reason that GeTe could not have become paraelectric well before the energy gap closed. The difference in those cohesive energies is also the difference between the total energies and therefore (according to Table III) at a unit cell volume of about  $46.50 \text{ \AA}^3$  (a reduction of 8.75% of the equilibrium volume), where the cohesive energy curves cross, is a first estimate for the point where the phase transition occurs. Our conclusion would be different if the 0.059 meV increase in the trigonal cohesive energy with the more stringent force criterion at the equilibrium volume were to apply at the transition volume. We used the same stringent criterion at the 9% volume reduction and found a trigonal cohesive energy increase of only 0.002 meV. VASP allows one to pick a force criterion and the code then picks a commensurate stress criterion. The former seems satisfactory as  $\tau(a)$  converges to 0.0 but the latter does not, as  $\alpha$  does not converge to  $90^\circ$ . To get the critical pressure we fit  $E_c^{\text{trig}}$  with a ninth order spline and obtained 5.65 GPa at the 8.75%

TABLE V. Comparison of enthalpy vs energy based critical parameters. The latter are distinguished by a “o” subscript.

	$H$ (eV)	$p_c$ (GPa)	$V_{\text{trig}}$ ( $\text{\AA}^3$ )	$V_{\text{cube}}$ ( $\text{\AA}^3$ )	$\Delta V$ ( $\text{\AA}^3$ )	$E$ (eV)	$p_{\text{co}}$ (GPa)	$V_{\text{co}}$ ( $\text{\AA}^3$ )
LDA	-6.1601	5.313	46.7582	46.6683	0.0899	7.7005	5.417	46.7201
GGA	-3.7559	8.448	47.6777	47.6138	0.0639	6.2761	8.523	47.6568

reduction in the unit cell volume. After fitting  $E_c^{\text{cube}}$ , the ninth order spline resulted in an 8.32% reduction in volume at the cubic and trigonal energy spline curves' crossover point at which point the critical pressure was 5.42 GPa. The difference between these two critical pressures can be taken as an estimate of the uncertainty in our results. The latter results are listed in Table V with an “o” subscript for comparison with the enthalpy minimization results. A Vinet<sup>17</sup> fit resulted in a 14.81% volume reduction at the crossover point and a 9.71 GPa critical pressure and thus was not further considered.<sup>26</sup>

To calculate  $H=E+pV$ , for both the cubic and trigonal phases, we took their  $E(V)$  fits and derivatives of the fits,  $p$ , to obtain  $H(p)$  at the 22 volumes listed in Table III. These  $H(p)$  were fit with the nine point spline. The pressure at which the two spline curves cross is the critical pressure which is listed in Table V along with the cubic and trigonal volumes at the critical pressure. The results differ only slightly, and in the direction expected, from those obtained from equating the energies. The transition is first order, but only barely, with a volume discontinuity of 0.19%. Note also that  $V_{\text{trig}} > V_o > V_{\text{cube}}$ , as expected. The critical pressure of 5.313 GPa is only 0.104 GPa less than  $p_{\text{co}}$  which is much less than the uncertainty previously discussed. The GGA vol-

ume discontinuity is only 0.134% and its critical pressure only 0.075 GPa below  $p_{\text{co}}$ .

To recapitulate, using both the LDA and GGA, we calculated many of the ground state properties of rhombohedral GeTe. Except for the energy gap where the LDA was in near perfect agreement with the experiment, the LDA and GGA results were on opposite sides of the experimental values. There are no experimental values for the polarization where the LDA and GGA results were unexpectedly large, but in good agreement with each other and with other ferroelectrics. From the polarization we obtained the Born effective charge which was correspondingly large. We then calculated most of these properties as a function of volume as well as some for the rock salt structure to find the volume and pressure at which the trigonal to rock salt transition occurs. We found that for both LDA and GGA the phase transition is first order, but with a volume discontinuity that may be too small to measure, and that it occurred at a pressure close to that at which the energy gap vanishes.

This work was supported by the Welch Foundation (Houston, TX) under Grant No. F-0934, and by the Texas Advanced Computing Center. B.R.S. was supported by the DARPA AP2C program.

<sup>1</sup>M. Chen, K. A. Rubin, and R. W. Barton, Appl. Phys. Lett. **49**, 502 (1986).

<sup>2</sup>T. Chattopadhyay, J. X. Boucherle, and H. G. von Schnering, J. Phys. C **20**, 1431 (1987).

<sup>3</sup>K. M. Rabe and J. D. Joannopoulos, Phys. Rev. B **36**, 6631 (1987).

<sup>4</sup>J. M. Leger and A. M. Redon, J. Phys.: Condens. Matter **2**, 5655 (1990).

<sup>5</sup>N. R. Serebryanaya, V. D. Blank, and V. A. Ivdenko, Phys. Lett. A **197**, 63 (1995).

<sup>6</sup>S. S. Kabalkina, L. F. Vereshchagin, and N. R. Serebryanaya, Sov. Phys. JETP **24**, 917 (1967).

<sup>7</sup>A. Onodera, I. Sakamoto, Y. Fujii, N. Mori, and S. Sugai, Phys. Rev. B **56**, 7935 (1997).

<sup>8</sup>I. A. Kornev, L. Bellaiche, P. Bouvier, P.-E. Janolin, B. Dkhil, and J. Kreisel, Phys. Rev. Lett. **95**, 196804 (2005).

<sup>9</sup>C. M. I. Okoye, J. Phys.: Condens. Matter **14**, 8625 (2002).

<sup>10</sup>P. E. Blöchl, Phys. Rev. B **50**, 17953 (1994).

<sup>11</sup>G. Kresse and J. Furthmüller, Phys. Rev. B **54**, 11169 (1996); Comput. Mater. Sci. **6**, 15 (1996).

<sup>12</sup>J. P. Perdew, K. Burke, and M. Ernzerhof, Phys. Rev. Lett. **77**, 3865 (1996).

<sup>13</sup>P. E. Blöchl, O. Jepsen, and O. K. Andersen, Phys. Rev. B **49**,

16223 (1994).

<sup>14</sup>The VASP code picks a stress criterion consistent with the selected force criterion but does not reveal it.

<sup>15</sup>The primitive fcc lattice vector  $(a/2, a/2, 0)$  becomes  $[(1 + \epsilon)a/2, (1 + \epsilon)a/2, \epsilon a]$  under the trigonal distortion. The fcc  $(a, 0, 0)$  becomes  $(a, \epsilon a, \epsilon a)$ . The VASP code calculates the former, from which the components of the latter are easily obtained. Our LDA values for  $(1 + \epsilon)a/2$  and  $\epsilon a$  are 5.89897 and 0.033243 Å, respectively.

<sup>16</sup>Charles Kittel, *Introduction to Solid State Physics*, 7th ed. (Wiley, New York, 1996).

<sup>17</sup>The VASP code subtracts spin unpolarized atomic energies from the crystal total energy to obtain an incorrect value of the cohesive energy. We have substituted LDA and GGA spin polarized atomic energies obtained from supercell calculations.

<sup>18</sup>P. Vinet, J. Ferrante, J. H. Rose, and J. R. Smith, J. Geophys. Res. **92**, 9319 (1987).

<sup>19</sup>B. R. Sahu and Leonard Kleinman, Phys. Rev. B **72**, 113106 (2005).

<sup>20</sup>L. L. Chang, P. J. Stiles, and L. Esaki, IBM J. Res. Dev. **10**, 484 (1966).

<sup>21</sup>J. C. Slater, *Symmetry and Energy Bands in Crystals* (Dover, New York, 1965), p. 418.

- <sup>22</sup>R. D. King-Smith and D. Vanderbilt, Phys. Rev. B **47**, 1651 (1993).
- <sup>23</sup>Tanaka and K. Shindo, J. Phys. Soc. Jpn. **50**, 3349 (1981).
- <sup>24</sup>Actually,  $Z^*$  is the longitudinal (i.e., along the three-fold axis) component of a two component tensor.
- <sup>25</sup>Since  $Z^*$  depends on the derivative of the polarization, a large  $Z^*$  can occur even if there is no polarization. A crude estimate of the derivative of the polarization may be obtained from  $P/\tau$  and results in  $Z^* = 15.22$  (LDA).

<sup>26</sup>The various EOS have only four parameters, the equilibrium volume, energy, bulk modulus, and its derivative. That four parameters, involving only the energy minimum, can fit the entire  $E(V)$  curve as well as they do is impressive but because  $E_c^{\text{cube}}$  and  $E_c^{\text{trig}}$  are so nearly parallel around their crossing point, the EOS fits are incapable of finding the crossing point accurately. The nine point spline, because it has no EOS assumptions built into it, yields much more accurate fits.